The Effects of Estrogen and Chemotherapy on the Dynamics of Malignant Breast Cancer on

Cindy C. Jackson[1], Lindsey K. Lauderdale[2], Nicholas Earl Millett[3], Samantha Anne Smee[4], and Adrian Smith[5]

[1] Department of Mathematics and Statistics, California State Polytechnic University

Pomona, CA 91768, USA.

[2] Department of Mathematics, University of Illinois at Urbana-Champaign

Urbana, IL 61801, USA.

[3] Department of Mathematics and Statistics, The University of Maine

Orono, ME 04469, USA.

[4] Department of Mathematics, Oregon State University

Corvallis, OR 97331, USA.

[5] Department of Mathematics, University of Washington

Seattle, WA 98195, USA.

August 2008

Abstract

Here we present two mathematical models each of which is used to examine two different drug treatment regimens on estrogen receptor-positive breast cancer in women. The first regimen is a combination therapy of estrogen stimulation followed by chemotherapy and the second regimen is a treatment of chemotherapy alone. The method under consideration is to first use estrogen therapy on a patient diagnosed with breast cancer to move the tumor cells into the proliferating stage, at which time chemotherapy can be applied to kill the proliferating cancer cells. Utilizing both analytical and numerical approaches, a study of the efficacy of combination treatment and the single treatment is completed. Two partially decoupled models are created to study both a healthy cell population and a cancerous cell population in the breast. At first, the cancerous cell population (tumor growth) is analyzed separately from the healthy cell population, then later composed with the healthy cell model to examine the dynamics of cancer and treatment on the body. Both of the populations are divided into quiescent and proliferating stages in order to account for the cell cycle specific treatment that are later applied. According to the constructed models, the treatment regimen consisting of chemotherapy alone is more effective in eliminating the tumor cell population than the regimen consisting of both estrogen chemotherapy.

A Introduction

A.1 Background

Cancer is one of the major health problems facing the world today, accounting for approximately thirteen percent of deaths worldwide [?] [?]. There are many different forms of cancer, however breast cancer affects women of all ages, races, and genetic backgrounds [?] [?]. It is the second most common form of cancer, comprising roughly eleven percent of cancer diagnoses [?] [?]. In the United States, breast cancer affects one out of every eight women and is the second highest cause of cancer fatality, with approximately 40,500 deaths per year [?]. Over 258,000 women are diagnosed with breast cancer in the United States alone [?]; this cancer has become a growing epidemic [?]. With such a devastating impact on society, research into effective treatment of breast cancer is an ongoing process, which is vital to our health.

Breast cancer is an abnormal growth of cells in the breast tissue [?] [?]. It usually begins in the milk ducts of the breasts, and can eventually become a tumor. There are many types of cancerous tumors which occur

in the breast, the most common type being a ductal carcinoma [?]. In many cases, carcinomas occurring in the breast are tumors which are estrogen-receptor positive. These types of tumors have an excess of estrogen receptors making them extremely sensitive to the presence of estrogen. When estrogen is present, the tumorous cells are stimulated to proliferate [?]. As a result, estrogen-receptor positive ductal carcinomas are responsive to estrogen treatment, a treatment designed to push quiescent tumor cells into proliferation.

A.2 Cancer and the Cell Cycle

The cell cycle consists of five main phases. Four of these are proliferating stages, where the cell is in the act of dividing, and one quiescent or dormant stage. The proliferating stages are G_1, S, G_2, and M[?]:

- The G_1 phase, or gap phase 1, is where the cell begins to grow and synthesize different enzymes in preparation for DNA synthesis[?].
- The S phase begins when the cell replicates its DNA, creating duplicates of its entire set of chromosomes[?].
- The third phase is the G_2 phase, also referred to as gap phase 2, where the cell again grows rapidly, repairing any damage that may have occurred during the S phase and synthesizing various proteins that are required for mitosis[?].
- The final stage is mitosis, M, where the cell separates its chromosomes into two identical sets, and then divides its nuclei, cytoplasm, organelles, and cell membrane into two new cells[?]. These cells are born back into the G_1 phase.

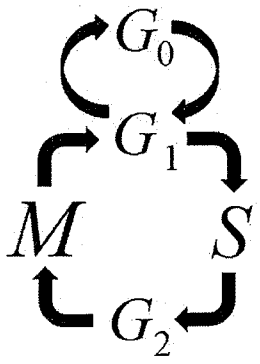

Figure 33: The cell cycle is a series of events that occur in both cancerous cells and healthy cells.

The quiescent, or non-proliferating, stage is called the G_0 stage. In this stage the cell is dormant or not actively dividing [?]. Cells enter the G_0 phase through a checkpoint in the G_1 phase. A cell can be moved into quiescence due to many factors, but usually due to lack of nutrients or space to grow [?]. Note that a majority of the cells in a healthy human body are in this phase.

During the normal division process, healthy cells are tightly regulated by the body so that they cooperate with each other and will collectively form various tissues [?]. At various stages in the cell cycle, the cell division process passes through checkpoints, where if the cell division process is malfunctioning, the cell cycle will stop and the cell will not continue dividing [?]. Cancer is a disease in which mutations occur in a way such that cancerous cells are no longer controlled at normal cell division checkpoints. As a result of these mutations, proteins and enzymes normally present in the cell which cause a cell to cease the division process in case of a failed checkpoint are not present [?]. Hence, cancerous cells often divide uncontrollably. Populations of uncontrollably dividing cells form tumors.

Though tumorous cells are not subject to normal cell division checkpoints, there are several factors that can limit the growth of a tumor. For example, due to the geometry of tumors, not all tumorous cells are proliferating at all times. Most tumors are made of various layered subunits. The outer layer of the tumorous subunit, being

exposed to a nutritious environment, consists of uncontrollably proliferating cells. Beneath the proliferating outer layer lies a layer of quiescent cells. These cells no not have sufficient nutrients to proliferate but do have sufficient nutrients to maintain a dormant state of life. This dormant stage of life corresponds to the G_0 stage of the cell cycle. At the innermost layer of the tumor subunit is a population of necrotic cells. Not only does this population of cells lack sufficient nutrients for proliferation, but they also lack the necessary nutrients for the maintenance of a dormant state of life. As a result, the necrotic center of the tumor subunit is made up of dead and dying cells.

The growth of a tumor subunit is due to the uncontrolled division of cells in the outermost layer. As these cells multiply more layers of cells are added to the outside of the tumor subunit. Due to the addition of cells to the outermost region of the tumor subunit, previously existing cells become further isolated form the nutrients necessary to maintain either proliferating or quiescent states. In particular, as layers of new cells are added to the outside of the tumor subunit, quiescent cells at the innermost region of the quiescent layer become necrotic, and proliferating cells at the innermost region of the proliferating layer become quiescent.

A.3 Treatment

Chemotherapy refers to the use of drugs to target cells for treatment. A systemic chemotherapy will affect the whole body by flowing through the bloodstream. Most chemotherapies are administered in cancer patients to specifically target cells that are actively dividing [?]. Chemotherapy works by either attaching to the cell during the S phase and interfering with DNA replication, or during the M phase, which disrupts the actual division of the cell. Both of these situations will cause the cell to die. While other chemotherapy can either block the enzymes cells need to survive and grow (in the case of cytostatic chemotherapy), or they can kill the cell as it is proliferating (called cytotoxic chemotherapy). Cells that are proliferating are vulnerable to chemotherapy treatment while quiescent cells are not. Unfortunately this chemotherapy does not specifically target cancer cells, but all of the cells in the body that are actively proliferating. Though the treatment is effective in killing cancer cells, steps must be taken to protect patients from its adverse effects on healthy tissue. The healthy cells that are affected the worst by chemotherapy are rapidly diving cells, such as those in the blood, mouth, and vagina. [?]

When treating breast cancer patients, estrogen is a common from of treatment and can only be effective in women who have tested positive for the for a response to hormone therapy [?]. Estrogen is a naturally occurring hormone that is responsible for secondary female sex characteristics, including breast development. During every menstrual cycle, with the help of other hormones, estrogen signals the cells in the breast to divide and multiply. In the case of estrogen receptor-positive breast cancer, it is the presence of estrogen that stimulates the tumor cells to continuously multiply [?]. Estrogen receptors are similar to antennae on a cancerous cell. The hormone will travel through the bloodstream and attach to the receptors, sending signals through the receptors telling the cells to grow and multiply [?]. Because cancerous cells are mutated they have a far greater amount of estrogen receptors than normal breast cells. Estrogen does not have an effect on proliferating cells, it can only signal the quiescent cells into proliferation.

B The General Model

In an effort to understand the dynamics of both cancerous and non-cancerous cells in the presence of drug and hormone treatments, a general mathematical model is constructed. Of particular interest is the comparison of a combined estrogen and chemotherapy treatment regimen to a treatment regimen consisting of chemotherapy alone. To account for the fact that estrogen and chemotherapy treatments are effective only at specific stages in the cell cycle, the general cell model is split into two compartments. One compartment consists of proliferating cells, the cells which are responsive to chemotherapy treatment, while the other consists of non-proliferating or quiescent cells, the cells which are responsive to estrogen treatment. This two-compartment cell model will be applied to populations of both healthy and cancerous cells. There are therefore four state variables, which are

- $N_T(t)$, the population size of quiescent (non-proliferating) tumor cells,
- $P_T(t)$, the population size of proliferating tumor cells,
- $N_H(t)$, the population size of quiescent healthy (non-proliferating) cells, and
- $P_H(t)$, the population size of proliferating healthy cells.

The general form of the model is

$$\dot{N_T}(t) = f_T(N_T, P_T) - g_T(P_T) - e_T N_T - d_T N_T \quad (1)$$

$$\dot{P_T}(t) = g_T(P_T) - f_T(N_T, P_T) + e_T N_T + \gamma_T P_T - c P_T \quad (2)$$

$$\dot{N_H}(t) = f_H(N_T, P_T, N_H, P_H) - g_H(P_T, P_H) - d_H N_H \quad (3)$$

$$\dot{P_H}(t) = g_H(P_T, P_H) - f_H(N_T, P_T, N_H, P_H) + \gamma_H P_H - c P_H, \quad (4)$$

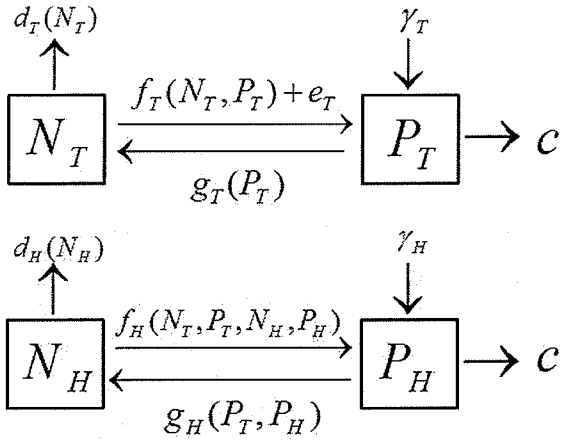

Figure 34: This is a template for the general model. Note that the tumor cells are independent of the healthy cells.

where f_T, g_T, f_H and g_H are functions describing the rates of migration of cells between proliferating and non-proliferating classes, and d_T, d_H are functions describing the death rates of quiescent cells due to both necrosis and apoptosis. In particular, f_T and f_H describe the non-hormone induced rates of migration of cells from the quiescent class to the proliferating class for the tumorous cells and the healthy cells respectively, while g_T and g_H are functions describing the respective rates of migration of cells from the proliferating stage to the non-proliferating stage for tumorous and healthy cells. The rate of estrogen induced movement of cancerous cells from quiescence to proliferation is assumed to be proportional to the number of non-proliferating cancerous cells and is given by $e_T N_T$. The rates of death of proliferating cancerous and healthy cells due to chemotherapy are assumed to be proportional to the number of cells in the corresponding proliferating classes and are given by cP_T and cP_H respectively. Finally, proliferating cells contribute to the proliferating cell class via mitosis at rates γ_T and γ_H per cell for tumorous and healthy cells respectively.

C First Model

C.1 Description

In this model, the functions f_T, f_H, g_T, g_H, d_T and d_H from the general model are taken to be

$$f_T(N_T, P_T) = \nu_T \left(1 - \frac{N_T+P_T}{K_T}\right)$$

$$f_H(N_T, P_T, N_H, P_H) = \nu_H \left(1 - \frac{N_T+P_T+N_H+P_H}{K_H}\right)$$

$$g_T(N_T, P_T) = \omega_T \left(\frac{P_T}{K_T}\right)$$

$$g_H(P_T, P_H) = \omega_H \left(\frac{P_H+P_T}{K_H}\right)$$

$$d_T(N_T) = \mu$$

$$d_H(N_H) = d.$$

With these functions specified as above, the general equations (1), (2), (3), and (4) become

$$\dot{N_T}(t) = \omega_T P_T \left(\frac{P_T}{K_T}\right) - \nu_T N_T \left(1 - \frac{N_T+P_T}{K_T}\right) - e_T N_T - \mu N_T \quad (5)$$

$$\dot{P_T}(t) = \nu_T N_T \left(1 - \frac{N_T+P_T}{K_T}\right) + e_T N_T + \gamma_T P_T - \omega_T P_T \left(\frac{P_T}{K_T}\right) - cP_T \quad (6)$$

$$\dot{N_H}(t) = \omega_H P_H \left(\frac{P_H+P_T}{K_H}\right) - \nu_H N_H \left(1 - \frac{N_T+P_T+N_H+P_H}{K_H}\right) - dN_H \quad (7)$$

$$\dot{P_H}(t) = \nu_H N_H \left(1 - \frac{N_T+P_T+N_H+P_H}{K_H}\right) + \gamma_H P_H - \omega_H P_H \left(\frac{P_H+P_T}{K_H}\right) - cP_H. \quad (8)$$

The functions for this first model, are now broken down and analyzed term by term, to understand their biological significance. Migration between the two tumor cell stages is represented by $\nu_T N_T \left(1 - \frac{N_T+P_T}{K_T}\right)$ (from N_T to P_T) and $\omega_T P_T \left(\frac{P_T}{K_T}\right)$ (from P_T to N_T), with K_T being the carrying capacity of the tumor. Migration between the two healthy cell stages are represented by $\nu_H N_H \left(1 - \frac{N_T+P_T+N_H+P_H}{K_H}\right)$ (from N_H to P_H) and $\omega_H P_H \left(\frac{P_T+P_H}{K_H}\right)$ (from P_H to N_H), with K_H being the carrying capacity of the cells in the breast. The quiescent cells will begin proliferating to fill the space available or to use an abundance of nutrients. The parameters ν_T and ν_H are the constant rates of transfer from quiescence to proliferation, in the tumor and healthy cell populations respectively. Similarly, the constant rates of proliferating cells moving back to quiescence due to limiting nutrients and space are ω_T and ω_H for the tumor and healthy cell populations. The probabilities $\left(\frac{P_T}{K_T}\right)$ (tumor cell population) and $\left(\frac{P_H+P_T}{K_H}\right)$ (healthy cell population) represent the event any one proliferating cell will move to the quiescent class. The mitotic rate of growth of the proliferating tumor cell population is $\gamma_T P_T$, while the mitotic rate of growth of the healthy cell population is $\gamma_H P_H$. The death rate of quiescent cells due to apoptosis and necrosis in the tumor is μN_T while dN_H only accounts for apoptosis in the healthy cell population. The treatment is accounted for in equations (5), (6), and (8) by the terms $e_T N_T$, cP_T, and cP_H. The rate which estrogen treatment is able to progress quiescent tumor cells to move to proliferation is $e_T N_T$, while the terms cP_T and cP_H represent the respective rates at which tumor and healthy cells are removed from the system by chemotherapy.

C.2 Analysis

The system is being analyzed in two parts. First, the tumor cells which are described by equations (5) and (6) are analyzed followed by the analysis of the healthy cells whose dynamics are governed by equations (7) and

(8). Note that equations (5) and (6) do not contain any of the healthy cell state variables. Therefore, analysis of two separate two dimensional systems, as opposed to one four dimensional system is justified. To investigate the stability of the system's equilibrium, the Jacobian is calculated. The Jacobian for the system is:

$$J_T(N_T, P_T) = \begin{pmatrix} -\mu - e_T + \frac{\nu_T N_T}{K_T} - \nu_T\left(1 - \frac{N_T + P_T}{K_T}\right) & \frac{\nu_T N_T}{K_T} + \frac{2\omega_T P_T}{K_T} \\ -\frac{\nu_T N_T}{K_T} + \nu_T\left(1 - \frac{N_T + P_T}{K_T}\right) & -c - \frac{\nu_T N_T}{K_T} - \frac{2\omega_T P_T}{KT} + \gamma_T \end{pmatrix}$$

By inspection, one can see that the two dimensional tumor system has a trivial equilibrium $(N_T, P_T) = (0, 0)$. This Jacobian evaluated at $(0, 0)$ is

$$J_T(0,0) = \begin{pmatrix} -\nu_T - \mu - e_T & 0 \\ \nu_T & -c + \gamma_T \end{pmatrix}.$$

Since $J_T(0,0)$ is lower triangular, the eigenvalues λ_1 and λ_2 are the diagonal entries. Hence, $\lambda_1 = -\nu_T - e_T - \mu$ and $\lambda_2 = -c + \gamma_T$. Since all parameter values are positive, the equilibrium $(0, 0)$ will be stable whenever $c > \gamma_T$. This condition is biologically interpreted as the rate of death of tumor cells from chemotherapy must be greater than the rate of new tumor cell production due to mitosis.

Given the independence of equations (5) and (6) on N_H and P_H and the stability properties of $(N_T, P_T) = (0, 0)$ in the two dimensional system (5) and (6), insight on the local stability properties of $(N_T, P_T, N_H, P_H) = (0, 0, 0, 0)$ can be gained by analyzing the two dimensional system (7),(8) in the case $(N_H, P_H) = (0, 0)$. In this case, equations (7) and (8) reduce to the same form as equations (5) and (6), and it is easily verified that the trivial healthy cell equilibrium $(N_H, P_H) = (0, 0)$ is locally asymptotically stable whenever $c > \gamma_H$. Thus, the trivial equilibrium is in the four dimensional system is locally asymptotically stable whenever $c > max(\gamma_H, \gamma_T)$ Of greater interest is the case $\gamma_T < c < \gamma_H$, which corresponds to stability of $(N_T, P_T) = (0, 0)$ and instability of $(N_H, P_H) = (0, 0)$. Both equilibrium will be investigated further in the second model.

C.3 Supercritical Hopf Bifurcation Analysis

Consider only the dynamics at the edge or boundary of the tumor mass, therefore analyzing the two dimensional tumor system. Using the substitutions $x = \frac{N_T}{K_T}$, $y = \frac{P_T}{K_T}$, and $t = d\tau$, equations (5) and (6) are rescaled as:

$$\dot{x}(\tau) = y^2 - ax\,(1 - (x + y)) - \alpha x, \qquad (9)$$
$$\dot{y}(\tau) = ax\,(1 - (x + y)) + \delta x + (b - \beta)\,y - y^2, \qquad (10)$$

where $a = \frac{\nu_T}{\omega_T}$, $b = \frac{\gamma_T}{\omega_T}$, $d = \frac{1}{\omega_T}$, $\alpha = \frac{e_T - \mu}{\omega_T}$, $\beta = \frac{c}{\omega_T}$, and $\delta = \frac{e_T}{\omega_T}$. Numerical analysis is performed using the parameter values in the following table:

	Values
a	4
b	10
α	20
β	varied
δ	10

As shown in section 3.2 the system has a trivial equilibrium at $(0, 0)$, which is locally asymptotically stable whenever $b < \beta$. Observe that this condition is equivalent to the condition $\gamma_T < c$, to so that in (9) and (10), $(x, y) = (0, 0)$ is locally asymptotically stable whenever the rate of death of proliferating cells is greater than the rate of introduction of cells into the proliferating class via mitosis. Note that in addition to the trivial equilibrium, there exists a non-trivial equilibrium given by:

$$x^* = \frac{(b\alpha - \beta\,\alpha + ab - a\beta)(b - \beta)}{-\beta\,\alpha + a\delta\,\beta + \beta\,\delta + a\alpha\,b - 2\,\delta\,\alpha + ab^2 - a\delta\,b + \delta^2 + \alpha^2 - a\alpha\,\beta - b\delta - 2\,ab\beta + b\alpha + a\beta^2}$$

$$y^* = \frac{-\beta\,\alpha^2+a\alpha\,b+b\alpha^2+a\delta\,\beta-b\alpha\,\delta+\beta\,\alpha\,\delta-a\delta\,b-a\alpha\,\beta}{-\beta\,\alpha+a\delta\,\beta+\beta\,\delta+a\alpha\,b-2\,\delta\,\alpha+ab^2-a\delta\,b+\delta^2+\alpha^2-a\alpha\,\beta-b\delta-2\,ab\beta+b\alpha+a\beta^2}$$

It can be shown that such each of $x*$ and $y*$ are positive precisely when both $\alpha > \delta$ and $b > \beta$. Observe that for positivity of both $x*$ and $y*$ to hold, the trivial equilibrium must be unstable. Through numerical simulations the existence of a Hopf bifurcation is determined. This means the non-trivial equilibrium (x^*, y^*) loses stability as the real parts of the complex conjugate eigenvalues of the Jacobian evaluated at (x^*, y^*) switch from negative to positive [?]. To show that this happens, the Jacobian is evaluated at the non-trivial equilibrium and the trace is obtained so that the first of two conditions for the existence of a supercritical Hopf bifurcation can be verified. To guarantee that the real parts of both eigenvalues are zero, the trace of of the Jacobian evaluated at the non-trivial equilibrium must be zero. That is the following equality must hold:

$$\alpha\,(b-\beta) + \frac{(-2\,a-2\,\alpha+a(b-\beta))(\alpha-\delta)}{b-\beta} + \frac{(-a-\alpha+b-\beta)(\alpha-\delta)^2}{(b-\beta)^2} = 0.$$

By further numerical investigation for fixed parameter values, it is discovered that the non-trivial equilibrium point changes stability at $\beta = 1.26$. The first Lyapunov coefficient is -.1164 and the system will undergo a supercritical Hopf bifurcation. Observe that varying β corresponds to varying chemotherapy since ω_T is fixed. If β is sufficiently large, for example $\beta = 10$, the non-trivial equilibrium does not exist and the trivial equilibrium is a stable node. As β is decreased the birth of a non-trivial equilibrium occurs. When born, this non-trivial equilibrium is a stable node and the trivial equilibrium loses stability. This loss of stability will occur by the time β has been decreased to 8. Further decreasing β to 6, causes the non-trivial equilibrium to switch stability from a stable node to a stable spiral. Finally, decreasing β from 6 to below 1.26 the non-trivial equilibrium becomes a stable limit cycle. Numerical methods suggest that this change in stability occurs for β near 1.26. Biologically this reflects at the boundary of the tumor there is a continual trade-off between the number of quiescent and proliferating cells. The number of proliferating cells will increase until they reach a limit due to limiting space and resources. As a result they are pushed back to a state of quiescence. This migration of proliferating cells back to the quiescent stage will result in an increase in quiescent cells to a point when quiescent cells out number the proliferating cells. As the quiescent cells migrate back to a state of proliferation the cycle begins again.

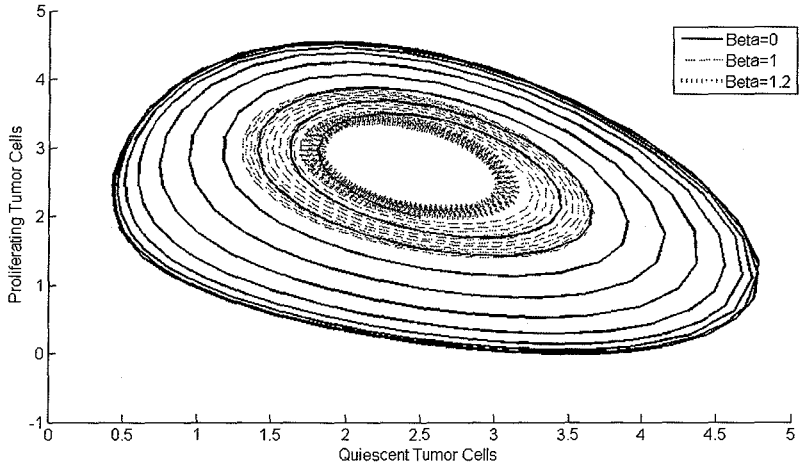

Figure 35: This Figure shows proliferating cells vs. quiescent cells. A stable limit cycle occurs when $\beta = 1.26$. The above images have $\delta = 10$, $\alpha = 20$, and β is varied. The system, for the given parameters, will not settle to equilibrium. The solutions will approach stable limit cycle. Without treatment, β=0, the tumor cells oscillate between proliferation and quiescence stages. This graph illustrates that as chemotherapy is increased the amplitude of the limit cycle decreases, i.e. effectively reducing the amount to tumor cells.

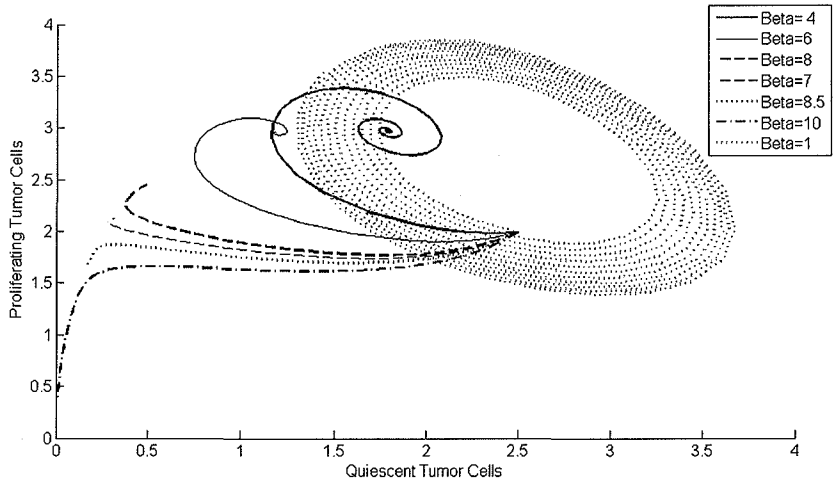

Figure 36: Here $\delta = 10$, $\alpha = 20$ and β is varied. If β is low the tumor cells will oscillate between proliferation and quiescence stages as seen by the limit cycle for β=1. As β is increased, the equilibrium will stabilize as we increase β through 1.26, this is indicative of a Hopf bifurcation. A further increase of β moves the stable equilibrium down until it coalesces with the origin. This graph illustrates that chemotherapy can stabilize the tumor equilibrium and ultimately bring the equilibrium to zero.

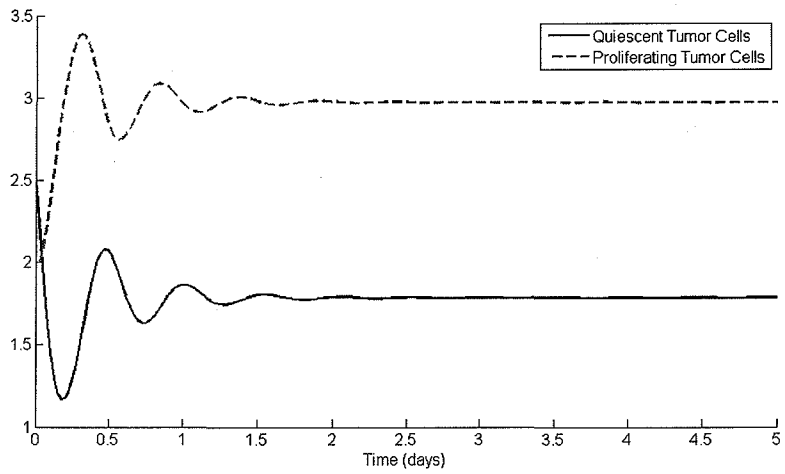

Figure 37: Here β=4, $\delta = 10$, and $\alpha = 20$. This graph illustrates that the proliferating cells and quiescent cells will converge to equilibrium. If chemotherapy is sufficiently large, the tumor cells will no longer oscillate but will stay constant.

C.4 Discussion

In the first model the main focus was on the two dimensional tumor system given by equations (1) and (2). In this system, the dynamics of quiescent cells and proliferating cells are incorporated in an attempt to investigate cell cycle specific chemotherapy. The chemotherapy targets and kills the tumor cells in proliferating cell stage only because the quiescent cells are not affected by the chemotherapy treatment. Through investigation and variation of the chemotherapy parameter c we were able to uncover several distinct qualitative behaviors of the tumor system. Local stability analysis gave the necessary condition for the existence of a stable cancer-free

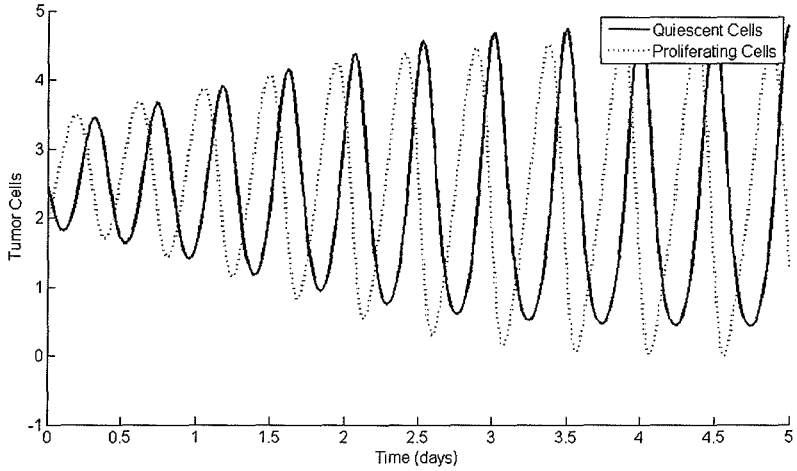

Figure 38: Here β=0, $\delta = 10$, and $\alpha = 20$. This graph illustrates that the proliferating cells and quiescent cells will exhibit self-sustained oscillations. At the boundary of the tumor mass there is a trade-off between the number of proliferating cells and quiescent cells.

equilibrium. This condition is $\gamma_T < c$, which says if the death rate due to chemotherapy is greater than the rate of proliferation or cell division, the tumor population will die out.

In order to investigate the non-trivial tumor equilibrium, the rescaled system in its non-dimensional form is considered. The rescaled chemotherapy parameter is $\beta = \frac{c}{\omega_T}$. Since ω_T is constant, varying β effectively varies the rate of chemotherapy introduced to the system. In the case of $\beta = 10$ representing high rate of chemotherapy, the non-trivial equilibrium coalesces with the cancer free equilibrium rendering it stable. While the amount of chemotherapy is reduced from $\beta = 10$ to $\beta = 8$, the trivial and the non-trivial equilibria become distinguished. In this case, the non-trivial equilibrium is a stable node, while the trivial equilibrium is unstable. While further reducing chemotherapy to $\beta = 6$, the non-trivial equilibrium switches stability type becoming a stable spiral. Administering chemotherapy from $1.26 < \beta < 6$, the non-trivial equilibrium remans a stable spiral but becomes more tightly coiled as β approaches 1.26 from above. At $\beta = 1.26$ the non-trivial equilibrium loses stability with the appearance of a stable limit cycle by Hopf bifurcation. This implies that the rate of death of proliferating cells due to chemotherapy is not high enough to keep the quiescent and proliferating tumor cells at a constant value. The amplitude of the limit cycle increases as β is further decreased all the way to zero. Biologically this reflects that at the boundary of the tumor there is a continual trade-off between the number of quiescent and proliferating cells. The number of proliferating cells will increase until they reach a limit due to limiting space and resources. As a result, some of the cells will be forced back to a state of quiescence. This migration of proliferating cells back to the quiescent stage will result in an increase in quiescent cells to a point when quiescent cells out number the proliferating cells. When enough space and nutrients become available the quiescent cells migrate back to a state of proliferation the cycle begins again.

Variations in chemotherapy give qualitative changes in the tumor equilibrium. For certain values of the chemotherapy parameter, the cyclic behavior of the quiescent and proliferating cells is stifled and if β is raised high enough the tumor population will not persist. This model can explain the qualitative behavior of the tumor growth when the tumor is very small. It explains how even at high levels of chemotherapy tumor persistence can be explained by this oscillating exchange at the boundary. This suggests that chemotherapy may not completely eliminate the tumor but can be used to prevent a larger tumor from recurring.

The first mathematical model was created in an effort to investigate two different treatment protocols; a combined chemotherapy and estrogen protocol and a protocol consisting of chemotherapy alone. While this model had interesting mathematical features and provided biological insight to the dynamics between proliferating and non-proliferating cells at the boundary of the tumor, it lacked the biological reality necessary to

provide any insight to the question. For example, numerical simulations showed that solutions can become negative, a result which is undesirable in any biological context. Because of this, a second mathematical model with more biologically realistic features is created. With a more precise model in place, the comparison of the two treatment protocols may be carried out.

D Second Model

D.1 Description

A new model is created in order to better examine the relationship between chemotherapy treatment and estrogen treatment. As in the general model, there is a class of tumor cells and a class of healthy cells, each class being divided into quiescent and proliferating stages. The state variables are the same as in the general model and the equations governing the dynamics of the tumor and healthy cells are:

$$\dot{N_T}(t) = \omega_T P_T \left(\frac{P_T}{K_T}\right) - \nu_T N_T \left(\frac{K_T}{2P_T+K_T}\right) - e_T N_T - \mu N_T \left(\frac{N_T}{K_T}\right) \quad (11)$$

$$\dot{P_T}(t) = \nu_T N_T \left(\frac{K_T}{2P_T+K_T}\right) + e_T N_T + \gamma_T P_T - \omega_T P_T \left(\frac{P_T}{K_T}\right) - P_T \quad (12)$$

$$\dot{N_H}(t) = \omega_H P_H \left(\frac{P_H+P_T}{K_H}\right) - \nu_H N_H \left(\frac{K_H}{2P_T+2P_H+K_H}\right) - dN_H \left(\frac{N_H}{K_H}\right) \quad (13)$$

$$\dot{P_H}(t) = \nu_H N_H \left(\frac{K_H}{2P_T+2P_H+K_H}\right) + \gamma_H P_H - \omega_H P_H \left(\frac{P_H+P_T}{K_T}\right) - cP_H. \quad (14)$$

Hence, the functions f_T, f_H, g_T, g_H, d_T and d_H in the general model are given by

$$f_T(N_T, P_T) = \nu_T \left(\frac{K_T}{2P_T+K_T}\right)$$

$$f_H(N_T, P_T, N_H, P_H) = \nu_H \left(\frac{K_H}{2P_T+2P_H+K_H}\right)$$

$$g_T(N_T, P_T) = \omega_T \left(\frac{P_T}{K_T}\right)$$

$$g_H(P_T, P_H) = \omega_H \left(\frac{P_H+P_T}{K_H}\right)$$

$$d_T(N_T) = \mu \left(\frac{N_T}{K_T}\right)$$

$$d_H(N_H) = d \left(\frac{N_H}{K_H}\right).$$

The functions for this first model, are now broken down and analyzed term by term, to understand there biological significance. Migration between the two tumor cell stages is represented by $\nu_T N_T \left(\frac{K_T}{2P_T+K_T}\right)$(from N_T to P_T) and $\omega_T P_T \left(\frac{P_T}{K_T}\right)$ (from P_T to N_T), with K_T being the carrying capacity of the tumor. And migration between the two healthy cell stages are represented by $\nu_H N_H \left(\frac{K_H}{2P_T+2P_H+K_H}\right)$ (from N_H to P_H) and $\omega_H P_H \left(\frac{P_T+P_H}{K_H}\right)$ (from P_H to N_H), with K_H being the carrying capacity of the cells in the breast. The quiescent cells will begin proliferating to fill the space available or to use an abundance of nutrients. The variables ν_T and ν_H are the constant rates of transfer from quiescence to proliferation, in the tumor and healthy cell populations respectively. Similarly, the constant rates of proliferating cells moving back to quiescence due to limiting nutrients and space are ω_T and ω_H for the tumor and healthy cell populations. The probabilities $\left(\frac{P_T}{K_T}\right)$ (tumor cell population) and $\left(\frac{P_H+P_T}{K_H}\right)$ (healthy cell population) represent the event any one proliferating cell will move to the quiescent class.

Similarly, the rates of this model are incorporated, to make the model biological realistic. The rate of growth of the tumor population is $\gamma_T P_T$, which is motivated by mitotic cancerous cells. While the rate of growth, due to mitosis of the healthy cell population is $\gamma_H P_H$. The death rate of quiescent cells due to apoptosis and necrosis in the tumor is $\mu N_T \left(\frac{N_T}{K_T}\right)$, where $\left(\frac{N_T}{K_T}\right)$ is the probability that any one cell in the quiescent stage will die. The term $dN_H \left(\frac{N_H}{K_H}\right)$ only accounts for apoptosis in the healthy cell population, where $\left(\frac{N_H}{K_H}\right)$ is the probability that any one cell in the quiescent stage will die. The treatment is accounted for in equations (11), (12), and (14) by the terms $e_T N_T$, cP_T, and cP_H. The rate which estrogen treatment is able to progress quiescent tumor cells to move to proliferation is $e_T N_T$. The variables cP_T and cP_H represent the respective rates at which tumor and healthy cells are removed from the system by chemotherapy.

D.2 Analysis

As in the first model, the second system will be analyzed in two parts. First, consider the tumor cell system equations (11) and (12). To investigate the local stability of the system's equilibrium, the Jacobian is calculated. The Jacobian for the system is:

$$J_T = \begin{pmatrix} -2\frac{\mu N_T}{K_T} - e_T - \frac{K_T \nu_T}{K_T + 2P_T} & \frac{2K_T \nu_T N_T}{(K_T + 2P_T)^2} + \frac{2\omega_T P_T}{K_T} \\ \\ \frac{K_T \nu_T}{K_T + 2P_T} + e_T & -\frac{2K_T \nu_T N_T}{(K_T + 2P_T)^2} - \frac{2\omega_T P_T}{K_T} - c + \gamma_T \end{pmatrix}.$$

The system has a trivial equilibrium $(N_T, P_T) = (0, 0)$. Evaluating the Jacobian at $(0, 0)$ gives

$$J_T(0,0) = \begin{pmatrix} -\nu_T - e_T & 0 \\ \nu_T + e_T & -c + \gamma_T \end{pmatrix}.$$

By inspection, the eigenvalues are $\lambda_1 = -\nu_T - e_T$ and $\lambda_2 = -c + \gamma_T$. Since each of the parameters are positive, the trivial equilibrium $(0, 0)$ will be stable whenever $c > \gamma_T$ and will be a saddle point whenever $c < \gamma_T$. Specifically, if there is no chemotherapy then $(0, 0)$ will be unstable. This means that if the total number of cancerous cells is positive and sufficiently small, the amount of cancerous cells in the body is growing. The non-trivial equilibria for the system (11), (12) are difficult to find analytically, so a numerical approach is taken. This will be discussed in section D.4.

Now consider the healthy cell system, equations (13) and (14). In the case of no cancer cells ($N_T = P_T = 0$) equations (13) and (14) reduce to the same forms as (11) and (12), with the exception of the estrogen term. In this case, the healthy cell system has a trivial equilibrium $(N_H, P_H) = (0, 0)$. The Jacobian of the healthy cell system with $(N_T, P_T) = (0, 0)$ evaluated at the trivial equilibrium is

$$J_H(0,0) = \begin{pmatrix} -\nu_H & 0 \\ \nu_H & -c + \gamma_H \end{pmatrix}.$$

Since the tumor system is decoupled from the healthy system, the Jacobian of the four dimensional system evaluated at the origin is a block diagonal matrix with two by two blocks, $J_H(0, 0)$ and $J_T(0, 0)$. From this it is clear that $(0, 0, 0, 0)$ is locally, asymptotically stable, provided $c > \max(\gamma_T, \gamma_H)$. Of greater interest is the case $\gamma_T < c < \gamma_H$. This corresponds the extinction of the tumor cell population and the persistence of the healthy cell population. Due to analytical complications this point will be investigated numerically in section D.4.

D.3 Sensitivity Analysis

In an effort to understand the relationship between the non-trivial tumor equilibrium (N_T^*, P_T^*), and the treatment parameters c and e_T, a sensitivity analysis is performed. Using Maple, the sensitivity indices

$$S_\zeta = \frac{\zeta}{T^*} \frac{\partial T^*}{\partial \zeta}$$

are computed for $\zeta = c, e_T$, where $T^* = N_T{}^* + P_T{}^*$ is the total number of cancerous cells in the nontrivial tumor equilibrium. In order to obtain S_ζ as a function of ζ only, parameters values in S_ζ are taken from the table in D.4, with $c = 0$ for $\zeta = e_T$ and $e_T = 0$ for $\zeta = c$.

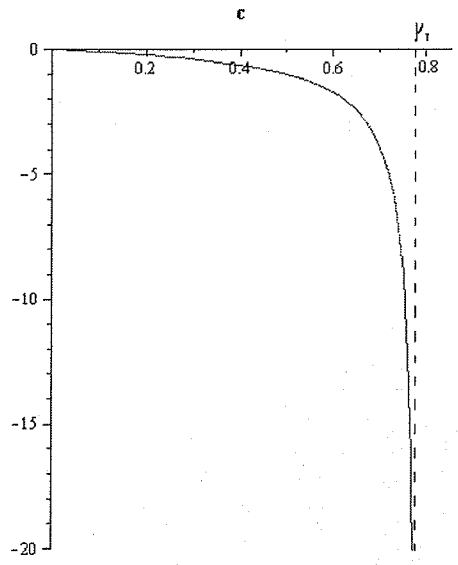

Figure 39: In the graph of S_c versus c from 0 to γ_T, the rate of chemotherapy treatment c and the sensitivity index S_c are negatively correlated. Observe that as $c \to \gamma_T$ from below, $S_c \to -\infty$. For c close to γ_T, T^* is more sensitive to small perturbations of c than if c is close to zero.

As shown in Figure 39, the rate of chemotherapy treatment c and the sensitivity index S_c are negatively correlated. In other words, as the rate of chemotherapy is increased, the non-trivial tumor equilibrium T^* decreases. Observe that as $c \to \gamma_T$ from below, $S_c \to -\infty$. For c close to γ_T, T^* is more sensitive to small perturbations of c than if c is close to zero. The asymptotic nature of S_c is in agreement with analytical results, as T^* only exists for $\gamma_T > c$. As $c \to \gamma_T$ from below, $T^* \to 0$, with T^* ceasing to exist for $\gamma_T \leq c$. Thus, for c near γ_T, small perturbations of c will cause relatively large changes in T^*.

Figure 40 shows a plot of S_{e_T} versus e_T. Observe that S_{e_T} is strictly increasing in e_T for $e_T \geq 0$. This implies for e_T close to zero, a small perturbation of e_T will cause a relatively small change in T^* than the same perturbation of e_T will cause when e_T is large. This is feasible in context because as the rate of estrogen therapy become sufficiently small, estrogen induced migration of quiescent tumorous cells into the proliferating class will be negligible relative to other form of migration into that same class. Therefore small perturbations of e_T will cause relatively small change in the migration rate of tumorous cells into the proliferation class and therefore small changes in the size of T^*. Oppositely, as the rate of estrogen therapy e_T becomes sufficiently large, estrogen induced migration of cells into the proliferation class becomes the dominant migration form for cells entering that class. Thus, for sufficiently large e_T, perturbations of e_T will have a much greater effect on the primary mode of migration, therefore greatly affecting the non-trivial tumor equilibrium T^*.

D.4 Numerical Analysis and Discussion

For the numerical analysis of this model, it was necessary to obtain accurate parameter values for the simulations. The following parameter values will be used:

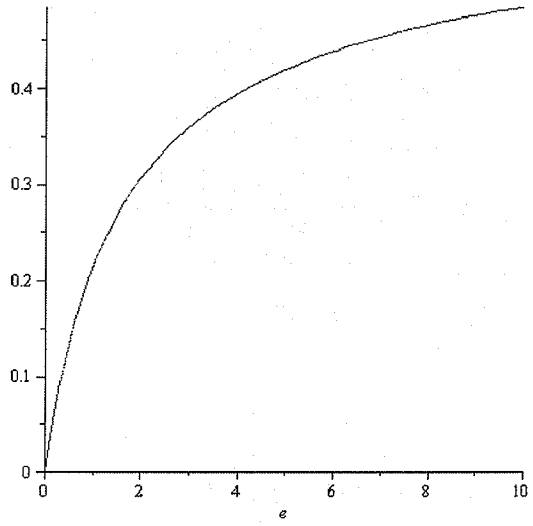

Figure 40: The graph of S_{e_T} versus e_T shows a plot of S_{e_T} versus e_T. Observe that S_{e_T} is strictly increasing in e_T for $e_T \geq 0$.

Parameter	Description	Value	Source
γ_T	Rate of Proliferation	.7869 day^{-1}	[?]
μ	Death Rate Due to Apoptosis and Necrosis	.07 + .477 = .547 day^{-1}	[?, ?]
ν_T	Maximum Rate of Migration from N_T to P_T	.9 day^{-1}	[?]
ω_T	Maximum Rate of Migration from P_T to N_T	.6 day^{-1}	[?]
K_T	Carrying Capacity of Proliferating Tumor Cells	3,088,118,000 cells	[?]
γ_H	Rate of Proliferation of Healthy Cells	1.47 day^{-1}	[?]
d	Death Rate Due to Apoptosis	.164 day $^{-1}$	[?]
ν_H	Maximum Rate of Migration from N_H to P_H	.48 day^{-1}	[?]
ω_H	Maximum Rate of Migration from P_H to N_H	5.643 day^{-1}	[?]
K_H	Carrying Capacity of the Healthy Cells	113,400,000,000 cells	[?, ?]

The values for most of these parameters come from previous models of tumor growth. However, the values for K_T and K_H were estimated from various data. K_T was found from the maximum possible tumor size, 2^{40} cells [3]. From the estimations assumed spherical geometry for the tumor and converted the cells to mm^3, using the conversion factor of 1 cell approximately equal to 10^{-6} mm^3[3]. Then we found the volume of a proliferating shell, approximately ten cells deep due to nutrient limitation, and converted that back to number of cells to estimate the parameter. The estimate for K_H was found in a similar fashion, though instead of using maximum tumor size, and average total breast volume was found[1]. This was converted to number of cells, then 20% (the typical proliferating fraction) of the number was used for K_H.

Because of the complexity of the nonzero equilibrium of our system, we must turn to numerical simulations to analyze the behavior of our system and the effects of the two treatments. Using our estimated parameter values, we find that for the 4-dimensional system, with no estrogen or chemotherapy treatment ($e = c = 0$), there are exactly three nonnegative equilibria. One is the origin $(0, 0, 0, 0)$, which (in the case of no treatment) is a saddle point, as we analyzed before. Examining the phase plane diagram, we see another is $(0, 0, N_H^\diamond, P_H^\diamond)$, which is a saddle point also. The third equilibrium $(N_T^*, P_T^*, N_H^*, P_H^*)$ is positive and stable (Figure 9).

If we introduce constant rate chemotherapy (no estrogen, so $e = 0$) we find that as the rate of chemotherapy increases, the positive equilibrium $(N_T^*, P_T^*, N_H^*, P_H^*)$ decreases until it coalesces with the four-dimensional trivial equilibrium. For the two-dimensional tumor cell system, as the rate of chemotherapy is increased, the nonzero tumor equilibrium moves closer to the origin until $(0, 0)$ becomes stable when $c > \gamma_T$, and similarly for the healthy cells (but when $c > \gamma_H$). Thus, $(0, 0, 0, 0)$ will be stable when $c > \max(\gamma_H, \gamma_T)$ (Figure 9)

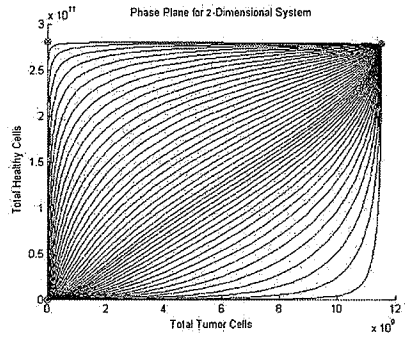

Figure 41: Phase plane diagram for the 4-dimensional system with no treatment. The horizontal axis is total tumor cells ($N_T + P_T$) and the vertical axis is total healthy cells ($N_H + P_H$). Note that (0,0) is seen to be a saddle point, and there exists a positive stable equilibrium.

D.4.1 Threshold for Healthy Cells

To measure the adverse effects of treatment protocols, we introduce a "threshold" for healthy cells. If the healthy cell population were to fall below this threshold, the cancer subject would be considered deceased or incurable, so this provides a limit as to how much chemotherapy the healthy cells can handle. As a theoretical example, we took a threshold of 30% of the cancer-free healthy cell equilibrium. In Figure 10, we look at the healthy and tumor cell equilibria as c varies from 0 to 1.8. We can see that the healthy cells remain above the threshold until about $c \approx 1.2$, and then they drop below (so the patient would be considered deceased).

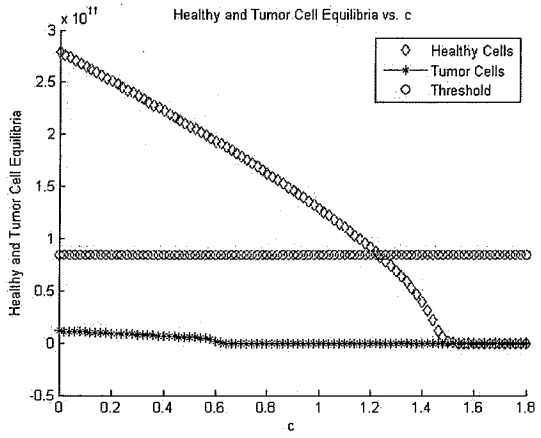

Figure 42: Healthy and tumor cell equilibria plotted against chemotherapy. The threshold is approximately 30% of the cancer free healthy cell equilibrium. We can see that the healthy cells remain above the threshold for $c <\approx 1.2$. Also note that we can see the tumor equilibrium change to zero at $c = \gamma_T = 0.7869$.

D.4.2 Combination vs. Single Treatment Protocol

With our threshold of healthy cells defined an estrogen/chemotherapy combination treatment protocol is compared to a treatment protocol involving just chemotherapy. In both treatment protocols, chemotherapy is 0.6.

The combination treatment calls for the application of estrogen ($e = 0.6$) for two days then chemotherapy is applied. The idea is to use estrogen to stimulate the quiescent tumor cells into proliferation thereby building a large class of tumor cells which are vulnerable to chemotherapy and then kill these vulnerable cells with chemotherapy. In Figure 13, the solid curve represents the the estrogen/chemotherapy combination treatment. The dashed curve represents the treatment protocol involving chemotherapy only. The cells first affected by estrogen die out slower than those to which only chemotherapy is applied. This indicates that using estrogen to first stimulate the cells into the proliferating class does not allow the chemotherapy to kill the cells more quickly after the estrogen is stopped.

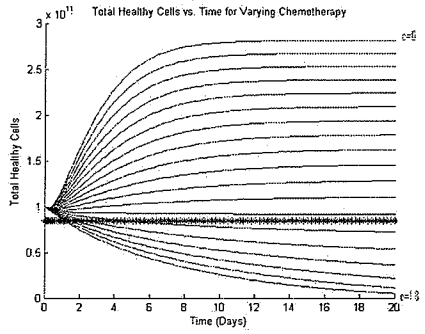

Figure 43: Healthy cell population ($N_H + P_H$) plotted against time as chemotherapy varies between 0 and 2.4. We can see that the healthy cell equilibrium decreases as the value of chemotherapy increases.

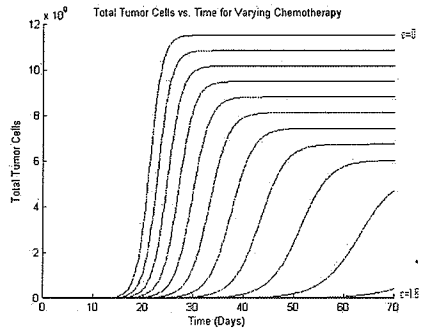

Figure 44: Tumor cell population ($N_T + P_T$) plotted against time as chemotherapy varies between 0 and 2.4. Here we also see that the tumor equilibrium decreases as the value of chemotherapy increases.

D.4.3 Constant Rate Chemotherapy vs. Periodic Chemotherapy

Since chemotherapy alone is the more effective of the two treatment protocols considered, we study the effects of a periodic chemotherapy treatment. In these simulations, constant rate chemotherapy is applied in discrete intervals with periods of no treatment in between. In Figure 14, the solid curve represents a treatment of $c = 2.4$ applied to the tumor cell population over intervals of 12 hours starting at $t = 0$. After 12 hours, the treatment is then stopped for another 12 hours, and then continued. The starred line is the tumor cells with constant chemotherapy $c = 1.2$. We can see that the two treatments have a similar effect on the tumor cells, killing them in about the same number of days. However, when we also look at the healthy cell population when subjected

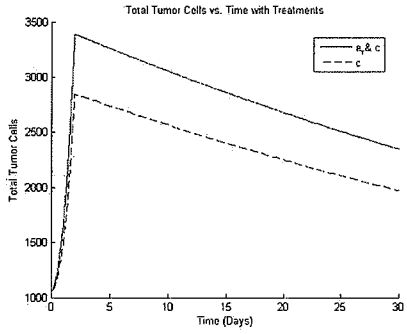

Figure 45: In this figure we look at the tumor cell population for combined estrogen and chemotherapy treatment. For the solid curve, constant estrogen is applied for 2 days and then switched to constant chemotherapy. For the dashed line, there is no treatment for the first two days, and then constant chemotherapy is applied. We can see that using estrogen to stimulate the cells does not enable the chemotherapy to kill the cells more quickly.

to the same treatments (Figure 15), we see that the healthy cells persist at a higher values when subjected to the periodic chemotherapy with $c = 2.4$, as opposed to the constant chemotherapy with $c = 1.2$. In both cases the healthy cells remain above the threshold. This indicates that this particular treatment protocol might be more effective than simply using constant chemotherapy, because it has a similar effect on the tumor cells but allows the healthy cells to persist at a higher population.

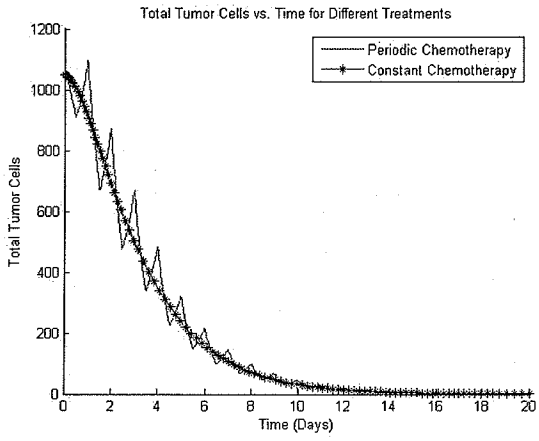

Figure 46: Tumor cell population ($N_T + P_T$) plotted against time as for periodic chemotherapy treatment. The solid line is periodic chemotherapy with $c = 2.4$ (in intervals of 12 hours) and the starred line is constant chemotherapy with $c = 1.2$. We set $c = 2.2$ and administered it in intervals of two days with a period of one day in between with no treatment. It can be seen that both treatments have similar effects.

Finally, there was an incorporation of a threshold for the healthy cells, to provide a limit which represents the minimum value of healthy cells that are needed for the cancer subject to remain alive. This threshold was purely theoretical and arbitrarily chosen, but provides a useful way to think about the balance between using chemotherapy to kill cancerous tumor cells and its detrimental effect on the healthy cell population. In the simulation, a threshold to be thirty percent of the cancer-free healthy cell equilibrium with no treatment was introduced. In this simulation a fixed chemotherapy rate was chosen in order to kill the tumor cells (so that $(0, 0)$ was stable for the tumor system), but the healthy cell population remained above the threshold. This

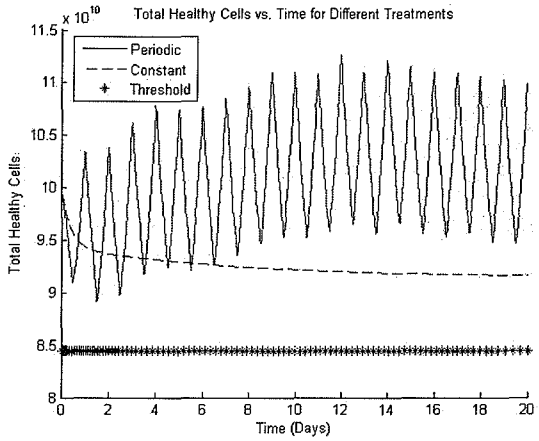

Figure 47: Healthy cell population ($N_H + P_H$) plotted against time as for the same periodic chemotherapy treatment as in Figure 9. It can be seen that with the periodic chemotherapy ($c = 2.4$) the healthy cells persist at higher values than for constant chemotherapy ($c = 1.2$).

corresponds to $\gamma_T < c < \gamma_H$ and stability of $((0, 0, N_H^*, P_H^*))$. If the rate of chemotherapy is increased, the cancer cells still approached zero and the healthy cells tended to a positive equilibrium, but below our proposed threshold. In such a case, even though the healthy cells did not die, the cancer patient would still be considered to be deceased and the treatment a failure.

E Conclusion

Two models for the tumor progression of breast cancer in women were constructed and analyzed. This was done in order to answer the question of which type of treatment was more effective: a combination therapy of chemotherapy and estrogen treatments or chemotherapy treatment alone. In both cases of the mathematical models, a system of four equations was created. The main focus of our attention was on the decoupled system representing the population of tumor cells. The first model discussed had very promising mathematics but at times lost biological meaning. In order to make the model more biologically accurate, it was modified. The migration rate from the quiescent stage to the proliferating stage of both the health and tumor cell populations was the major difference between the models. The second mathematical model had biological foundations and provided an answer to our question.

The original goal of this cancer model was to compare the dynamics of combined estrogen/chemotherapy treatment with chemotherapy alone and its effectiveness in decreasing the tumor size. The idea behind this treatment is that estrogen stimulates tumor cells from the quiescent stage into the proliferating stage where they are susceptible to chemotherapy. Simulations were run in which estrogen therapy was applied for two days and then stopped, at which time chemotherapy was added. This curve was then compared to one in which the cancer develops normally for two days and then is subjected to the same chemotherapy treatment as the first simulation. The results indicated that, contrary to our initial expectations, whenever estrogen is applied first to boost the proliferating cell count, applying chemotherapy then is always less effective in decreasing the tumor size than simply applying chemotherapy alone. Though the estrogen in fact does raise the number of proliferating cells, it appears that the chemotherapy does not succeed in killing these cells faster than those not treated with estrogen.

Once a treatment was obtained with the ability to effectively eliminate a tumor cell population, our focus turned to balancing the reduction of the tumor cell population with the adverse side affects of treatment. A theoretical measure of adversity of side affects of chemotherapy was introduced in the form of a threshold of number of healthy cells killed due to chemotherapy. Numerous treatment protocols were considered including

a constant rate chemotherapy treatment and a periodic chemotherapy treatment in which periods of constant rate chemotherapy were followed by periods of no chemotherapy. We found that while both constant rate chemotherapy and periodic chemotherapy had the ability to eliminate tumor cell populations without killing an undesirable number of healthy cells, periodic chemotherapy allowed healthy cells to persist at a higher level. In particular, given a constant rate chemotherapy treatment which eliminates a tumor population in a given amount of time, there is a periodic chemotherapy treatment consisting of short periods of high chemotherapy rates that can eliminate the tumor cell population in the same time. Moreover, for these two treatment regimens we find that the healthy cell population is able to persist at a higher level with the periodic chemotherapy treatment than with the constant rate chemotherapy treatment.

References

[1] Centers for Disease Control and Prevention. Achievements in Public Health, 1990-1999: Impact of Vaccines Universally Recommended for Children – United States, 1990-1998. *MMWR Morb Mortal Wkly Rep*, 48:241–248, 1999.

[2] Centers for Disease Control and Prevention. Ten Great Public Health Achievements - United States, 1900-1999. *MMWR Morb Mortal Wkly Rep*, 48:241–243, 1999.

[3] SL Plotkin and SA Plotkin. *Vaccines*, chapter 1, pages 1–12. W.B. Saunders Company, 3 edition, 1999.

[4] AB Coffield, MV Maciosek, JM McGinnis, JR Harris, MB Caldwell, SM Teutsch, D Atkins, JH Richland, and A Haddix. Priorities among recommended clinical preventive services. *American Journal of Preventive Medicine*, 21(1):1–9, 2001.

[5] WA Orenstein, RG Douglas, LE Rodewald, and AR Hinman. Immunizations in the united states: Success, structure, and stress. *Health Affairs*, 24(3):599–610, 2005.

[6] P Davies. Antivaccination web sites. *JAMA*, 288(14):1717–1718, Oct 2002.

[7] SP Calandrillo. Vanishing vaccinations: Why are so many americans opting out of vaccinating their children? *University of Michigan Journal of Law Reform*, 37:353–440, 2004.

[8] RT Chen. *Vaccines*, chapter 49, pages 1144–1163. WB Saunders Company, 3 edition, 1999.

[9] Centers for Disease Control and Prevention. Some Common Misconceptions about vaccination and how to respond to them. `http://www.cdc.gov/vaccines/vac-gen/6mishome.htm`, Accessed July 12, 2008.

[10] YA Maldonado. Current controversies in vaccination: Vaccine safety. *JAMA*, 288(24):3155–3158, 2002.

[11] A Wakefield, S Murch, A Anthony, J Linnell, D Casson, M Malik, M Berelowitz, A Dhillon, M Thomson, and P Harvey. Ileal-lymphoid-nodular hyperplasia, non-specific colitis, and pervasive developmental disorder in children. *The Lancet*, 351(9103):637–641, 1998.

[12] US Food and Drug Administration. Thimerosal in vaccines. `http://www.fda.gov/CbER/vaccine/thimerosal.htm`, Accessed July 8, 2008.

[13] E Gangarosa, A Galazka, C Wolfe, L Phillips, R Gangarosa, E Miller, and R Chen. Impact of anti-vaccine movements on pertussis control: the untold story. *The Lancet*, 351(9099):356–361, 1998.

[14] R Jacobson, P Targonski, and G Poland. A taxonomy of reasoning flaws in the anti-vaccine movement. *Vaccine*, 25(16):3146–3152, 2007.

[15] GA Poland and RM Jacobson. Understanding those who do not understand: a brief review of the anti-vaccine movement. *Vaccine*, 19:2440–2445, 2001.

[16] RM Wolfe. Content and design attributes of antivaccination web sites. *JAMA*, 287(24):3245–3248, 2002.

[17] RD Silverman. No more kidding around: Restructuring non-medical childhood immunization exemptions to ensure public health protection. *Annals of Health Law*, 12:277–294, 2003.

[18] J Thompson, S Tyson, P Cardhigginson, R Jacobs, J Wheeler, P Simpson, J Bost, K Ryan, and D Salmon. Impact of addition of philosophical exemptions on childhood immunization rates. *American Journal of Preventive Medicine*, 32(3):194–201, 2007.

[19] DA Salmon, M Haber, EJ Gangarosa, L Phillips, NJ Smith, and RT Chen. Health consequences of religious and philosophical exemptions from immunization laws: Individual and societal risk of measles. *JAMA*, 282(1):47–53, 1999.

[20] DA Salmon and AW Siegel. Religious and philosophical exemptions from vaccination requirements and lessons learned from conscientious objectors from conscription. *Public Health Reports*, 116(4):289–296, 2001.

[21] SB Omer, WKY Pan, NA Halsey, S Stokley, LH Moulton, AM Navar, M Pierce, and DA Salmon. Nonmedical exemptions to school immunization requirements: Secular trends and association of state policies with pertussis incidence. *JAMA*, 296(14):1757–1763, 2006.

[22] JG Hodge. School vaccination requirements: Legal and social perspectives. *NCSL State Legislative Rep*, 27:1–14, 2002.

[23] D Khalili and A Caplan. Off the grid: Vaccinations among homeschooled children. *The Journal of Law, Medicine & Ethics*, 35(3):1073–1105, Jul 2007.

[24] T May and RD Silverman. 'Clustering of exemptions' as a collective action threat to herd immunity. *Vaccine*, 21(11-12):1048–1051, 2003.

[25] A d'Onofrio, P Manfredi, and E Salinelli. Vaccinating behaviour, information, and the dynamics of SIR vaccine preventable diseases. *Theoretical Population Biology*, 71(3):301–317, 2007.

[26] A Maayan-Metzger, P Kedemfriedrich, and J Kuint. To vaccinate or not to vaccinate - that is the question: why are some mothers opposed to giving their infants hepatitis B vaccine? *Vaccine*, 23(16):1941–1948, 2005.

[27] A Wroe, A Bhan, P Salkovskis, and H Bedford. Feeling bad about immunising our children. *Vaccine*, 23(12):1428–1433, 2005.

[28] Thomas C. Schelling. *Micromotives and Macrobehavior*. W. W. Norton and Company, 1978.

[29] WO Kermack and AG McKendrick. A contribution to the mathematical theory of epidemics. *Proceedings of the Royal Society of London*, 115(772):700–721, 1927.

[30] JJ Gart. The mathematical analysis of an epidemic with two kinds of susceptibles. *Biometrics*, 24(3):557–566, 1968.

[31] F Ball. Deterministic and stochastic epidemics with several kinds of susceptibles. *Advances in Applied Probability*, 17(1):1–22, 1985.

[32] H Lacayo and NA Langberg. The exact and symptotic formulas for the state probabilities in simple epidemics with m kinds of susceptibles. *Journal of Applied Probability*, 19(1):1–9, 1982.

[33] CM Kribs-Zaleta and JX Valesco-Hernández. A simple vaccination model with multiple endemic states. *Mathematical Biosciences*, 164:183–201, 2000.

[34] S Rushton and AJ Mautner. The deterministic model of a simple epidemic for more than one community. *Biometrika*, 42(1-2):126–136, 1955.

[35] RK Watson. On an epidemic in a stratified population. *Journal of Applied Probability*, 9(3):659–666, 1972.

[36] NG Becker and K Dietz. The effect of household distribution on transmission and control of highly infectious diseases. *Mathematical Biosciences*, 127(2):207–219, 1995.

[37] F Ball, D Mollison, and G Scalia-Tomba. Epidemics with two levels of mixing. *Annals of Applied Probability*, 7(1):46–89, 1997.

[38] F Ball and P Neal. A general model for stochastic SIR epidemics with two levels of mixing. *Mathematical Biosciences*, 180:73–102, 2002.

[39] FG Ball, T Britton, and OD Lyne. Stochastic multitype epidemics in a community of households: Estimation of threshold parameter r and secure vaccination coverage. *Biometrika*, 91(2):345–362, 2004.

[40] RM Anderson RM May. Spatial heterogeneity and the design of immunization programs. *Mathematical Biosciences*, 72(1):83–111, 1984.

[41] DJ Murrell, U Dieckmann, and R Law. On moment closures for population dynamics in continuous space. *Journal of Theoretical Biology*, 229:421–432, 2004.

[42] D Hiebeler. Moment equations and dynamics of a household SIS epidemiological model. *Bulliten of Mathematical Biology*, 68(6):1315–1333, 2006.

[43] NG Becker and DN Starczak. Optimal vaccination strategies for a community of households. *Mathematical Biosciences*, 139(2):117–132, 1997.

[44] DH Zanette and M Kuperman. Effects of immunization in small-world epidemics. *Physica A: Statistical Mechanics and its Applications*, 309:445–452, 2002.

[45] Z Lu, X Chi, and L Chen. The effect of constant and pulse vaccination on SIR epidemic model with horizontal and vertical transmission. *Mathematical and Computer Modelling*, 36(9):1039–1057, 2002.

[46] PA Briss, LE Rodewald, AR Hinman, AM Shefer, RA Strikas, RR Bernier, VG Carande-Kulis, HR Yusuf, SM Ndiaye, and SM Williams. Reviews of evidence regarding interventions to improve vaccination coverage in children, adolescents, and adults. *American Journal of Preventive Medicine*, 18(1S):97–140, 2000.

[47] PA Gross, AW Hermogenes, HS Sacks, J Lau, and RA Levandowski. The Efficacy of Influenza Vaccine in Elderly Persons: A Meta-Analysis and Review of the Literature. *Annals of Internal Medicine*, 123(7):518–527, 1995.

[48] MJ Fine, MA Smith, CA Carson, F Meffe, SS Sankey, LA Weissfeld, AS Detsky, and WN Kapoor. Efficacy of pneumococcal vaccination in adults. A meta-analysis of randomized controlled trials. *Archives of Internal Medicine*, 154(23):2666–2677, 1994.

[49] J Ward, J Cherry, S Chang, S Partridge, and H Lee. Efficacy of an acellular pertussis vaccine among adolescents and adults. *New England Journal of Medicine*, 353(15):1555–1563, 2005.

[50] S Black, H Shinefield, B Fireman, E Lewis, P Ray, JR Hansen, L Elvin, KM Ensor, J Hackell, and G Siber. Efficacy, safety and immunogenicity of heptavalent pneumococcal conjugate vaccine in children. *The Pediatric Infectious Disease Journal*, 19(3):187, 2000.

[51] K O'Brien, L Moulton, R Reid, and R Weatherholtz. Efficacy and safety of seven-valent conjugate pneumococcal vaccine in American Indian children: group randomised trial. *The Lancet*, 362:355–361, 2003.

[52] N Becker. Estimation for discrete time branching processes with application to epidemics. *Biometrics*, 33(3):515–522, 1977.

[53] D Hiebeler. Populations on fragmented landscapes with spatially structed heterogeneities: Landscape generation and local dispersal. *Ecology*, 81(6):1629–1641, 2000.

[54] DE Hiebeler and AK Criner. Partially mixed household epidemiological model with clustered resistant individuals. *Physical Review E*, 75(2), 2007.

[55] O Diekmann, J Heesterbeek, and J Metz. On the definition and the computation of the basic reproduction ratio R_0 in models for infectious diseases in heterogeneous populations. *Journal of Mathematical Biology*, 28:365–382, 1990.

[56] K Dietz. The estimation of the basic reproduction number for infectious diseases. *Statistical Methods in Medical Research*, 2(1):23–41, 1993.

[57] J Li JM Hyman. An intuitive formulation for the reproductive number for the spread of diseases in heterogeneous populations. *Mathematical Biosciences*, 167:65–86, 2000.

[58] C Castillo-Chavez, JX Velasco-Hernandez, and S Fridman. Modeling contact structures in biology. *Frontiers of Theoretical Biology, Lecture Notes in Biomathematics*, 100:454–491, 1994.

[59] Ying-Hen Hsieh, P Driessche, and Lin Wang. Impact of travel between patches for spatial spread of disease. *Bull. Math. Biol.*, 69(4):1355–1375, May 2007.

[60] R Cohen, S Havlin, and D ben Avraham. Efficient immunization strategies for computer networks and populations. *Physical Review Letters*, 91(24):247901:1–4, 2003.

[61] M Murray and Z Rasmussen. Measles Outbreak in a Northern Pakistani Village: Epidemiology and Vaccine Effectiveness. *American Journal of Epidemiology*, 151(8):811–819, 2000.

[62] S van den Hof, CMA Meffre, MAE Conyn van Spaendonck, F Woonink, HE de Melker, and RS van Binnendijk. Measles Outbreak in a Community with Very Low Vaccine Coverage, the Netherlands. *Emerging Infectious Diseases*, 7(3 Supplement), 2000.

[63] J Puvimanasinghe, C Arambepola, and N Abeysinghe. Measles Outbreak in Sri Lanka, 1999-2000. *The Journal of Infectious Diseases*, 2003.

[64] C Stein-Zamir, N Abramson, H Shoob, and G Zentner. An outbreak of measles in an ultra-orthodox Jewish community in Jerusalem, Israel, 2007 - An in-depth report. *Eurosurveillance*, 13:1–4, 2008.

[65] JL Richard, V Masserey-Spicher, S Santibanez, and A Mankertz. Measles outbreak in Switzerland - An update relevant for the European football championship (EURO 2008). *Eurosurveillance*, 13(8), 2008.